Journal of University of Babylon, Engineering Sciences, Vol.(26), No.(5): 2018.

Behavior of Reinforced Concrete Hybrid Trapezoidal Box Girders Using Ordinary and Highly Strength Concrete

Nameer A. Alawsh **Teeba Haider Mehdi**
Civil Department, Engineering College,babylon of University
namer_alwash@yahoo.com tebahaider93@gmail.com

Abstract

In this paper, the general behavior of reinforced concrete hybrid box girders is studied by experimental and numerical investigation. Experimental work is included casting monolithically five specimens of box girders with trapezoidal cross section and testing it as simply supported under two point loading. Two specimens were cast as homogenous box girders (full normal strength concrete (NSC) (about 35 MPa) and full high strength concrete (HSC) (about 55 MPa)) and three specimens were cast as hybrid box girders (HSC in upper flange only, HSC in upper flange and half depth of webs, and HSC in bottom flange and total depth of webs). Experimental results showed significant effects of concrete hybridization on the structural behavior of box girders specimens such as: cracking loads, cracking patterns, ultimate strengths, and failure modes. The ultimate strength of Hybrid box girders increased by 23% as average when compared with the homogenous box girder (full NSC) and decreased by 9% as average when compared with homogenous box girder (full HSC). In numerical investigation, the tested specimens were modeled and analyzed using three dimensional non-linear finite element analysis. The analysis was carried out by using a computer program (ANSYS V16.1). The numerical results showed an acceptable agreement with the experimental work with difference about (3.12% and 9.588%) as average for ultimate load and deflection, respectively.

Key Words: Box Girder, Hybrid Concrete, Monolithic, Trapezoidal Cross section, HSC.

الخلاصة

تم في هذا البحث دراسة التصرف العام للروافد الخرسانية المسلحة ذات المقطع الصندوقي والمصنوعة من الخرسانة الهجينة (نوعين مختلفين من الخرسانة تصب ككتلة واحدة) عمليا ونظريا. تضمن الجزء العملي انشاء وفحص خمسة نماذج من الروافد الصندوقية مع مقطع شبه منحرف تحت تأثير فحص نقطي ثنائي التحميل. نموذجان من المقاطع الصندوقية تم صبهما من الخرسانة المتجانسة (احدهما من خرسانة عادية المقاومة (35 MPa) والاخر من خرسانة عالية المقاومة (٥٥ MPa)) وثلاثة نماذج من الخرسانة الهجينة (خرسانة عالية المقاومة في: الشفة العليا فقط، الشفة العليا ونصف عمق الوترة، و الشفة السفلى والعمق الكلي للوترة). بينت نتائج الدراسة العملية وجود تأثيرات مهمة لتهجين الخرسانة على التصرف الإنشائي لنماذج الروافد الصندوقية من حيث: احمال التشقق، نمط التشقق، المقاومات القصوى، و اشكال الفشل. المقاومة القصوى للروافد الصندوقية ذات الخرسانة الهجينة ازدادت بنسبة حوالي ٢٣% كمعدل بالمقارنة مع الروافد الصندوقية ذات الخرسانة المتجانسة (خرسانة عادية المقاومة) وقلت بنسبة حوالي ٩% فقط. في الجزء النظري من الدراسة تم تمثيل وتحليل النماذج المفحوصة بشكل رقمي باستخدام طريقة العناصر المحددة. النماذج الرقمية تم تكوينها بثلاثة أبعاد باستخدام برنامج إلكتروني (ANSYS الإصدار ١٦,١). أظهرت النتائج النظرية (التحليلية) توافقا معقولا مع النتائج العملية بنسبة اختلاف (٣,١٢% و ٩,٥٨٨%) كمعدل بالنسبة للحمل الاقصى والهطول، على التوالي.

الكلمات الافتتاحية: الرافدة الصندوقية، الخرسانة الهجينة، الصب الموحد، مقطع شبه المنحرف، الخرسانة عالية المقاومة.

1. Introduction and Background

Box girders are often used in Bridges due to their serviceability, stability, structural efficiency and construction economy. The reinforced concrete (RC) box girder consists of two webs that are joined by top and bottom flanges. The box shape is rectangular or trapezoidal in cross section. In addition, it can be constructed as a single cell, double cell or multi cell. When comparing box girder type with T-beam type, the box girder has more length span range that results in a lesser number of piers for the same width, which it is made box girder economic (Upadhyay and Maru, 2017).

The design and analysis of RC box girder are very complicated due to a combination of bending in longitudinal and transverse directions, torsion, and distortion. However, it is the most efficient cross-section.

The structural action when an external loads act on a box girder can be summarized it in the following:

1. Longitudinal flexural stresses and shear stresses across the section will result due to the simple beam action in the longitudinal direction.

2. The eccentricity of loading causes torsion of the cross section (St. Venant's shear stress) and distortion of the section that causes transverse bending stresses and longitudinal warping stresses.

The trapezoidal box girder provides a narrow bottom flange near the abutments where the bending moments is low. Also, a narrow flange of trapezoidal box girder allow frr steel savings (Paval, 2016).

Utilization of high strength concrete in the construction sector has increased due to its improved mechanical properties compared to ordinary concrete. The relatively recent development in concrete technology has led to produce high compressive strength concrete of (40 to 150 MPa). High strength concrete can be produced by adding high range water-reducing admixtures (Superplasticizer) and/or other admixtures (silica fume or fly ash) to Portland cement concrete (Newman and Choo, 2003).

Although high strength concrete offers advantages in terms of performance and economy of construction, the brittle behavior of the material remains a major drawback in some structural applications especially in earthquake resistant structures. Since the strength and ductility of concrete are inversely proportional, high strength concrete is significantly more brittle than the normal strength concrete (Ashour and Wafa, 1993). In order to overcome the problems in terms of deformability and ductility of concrete beams reinforced with steel bars, alternative solutions by using hybrid concrete concept is presented in this study.

2. Experimental Work

2.1 Description of Tested Specimens

2.1.1 Geometry and Reinforcement

The experimental program comprises of casting five RC box girders with trapezoidal cross section (the angle of inclined web with vertical axis was taken 2/1) and testing it as simply supported under two point loading. The test specimens were designed according to the specifications of (AASHTO, 2012). All the specimens had the same volume of concrete and the same amount of reinforcement. All specimens had the dimensions (2450 mm length, 200 mm overall depth, 800 mm width of upper flange, 550 mm width of bottom flange at bottom face of it, 70 mm thickness of webs and upper flange, and 60 mm thickness of bottom flange).

Also, all the specimens were reinforced by using bars of diameter 10 mm in the longitudinal direction in the bottom flange (ρ = 0.005) and upper flange and bars of diameter 6 mm in the transverse direction in bottom, upper flange and webs. Figure (1) shows the details of dimensions and reinforcement for the tested specimens.

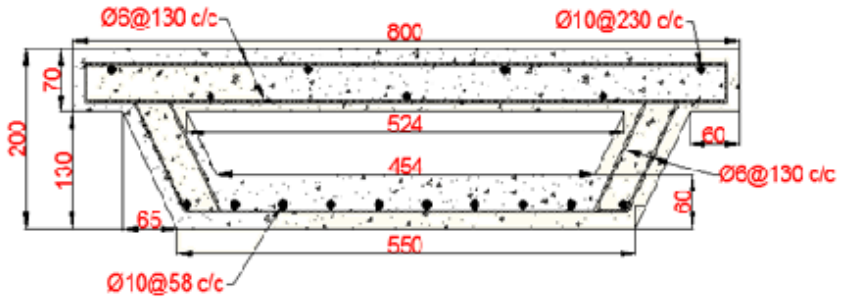

(a) Transverse section (typical trapezoidal cross section).

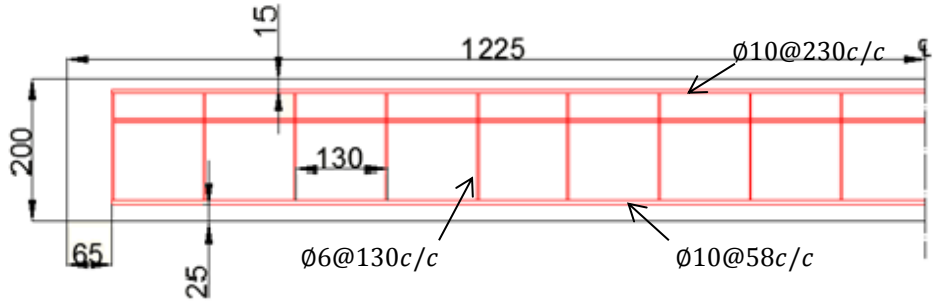

(b) Longitudinal section with symmetrical.

All Dimension in mm

Figure (1): Details of dimensions and reinforcement for the tested specimens.

2.1.2 Details of Tested Specimens (Cases Study)

The experimental work consisted of examining the use of different types of concrete strength (normal strength concrete (NSC) and high strength concrete (HSC)) in

the same specimen (hybrid section). Five specimens were cast monolithically, two of them were cast with homogenous concrete strength (full HSC and full NSC) and other three specimens were cast with hybrid strength concrete. Designations and details of box girders specimens are reported and presented in Fig. 2 as follows:

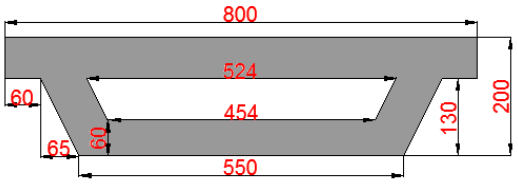

(a) T-HT

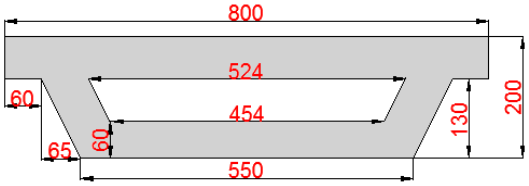

(b) T-NT

Normal Strength Concrete

High Strength Concrete All Dimensions in mm

Figure (2): Designations and details of testing specimens.

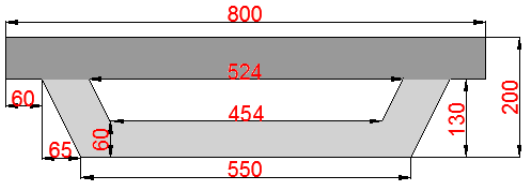

(c) T-HUF

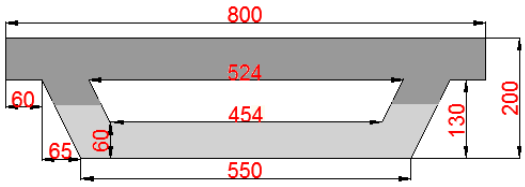

(d) T-HUF0.5W

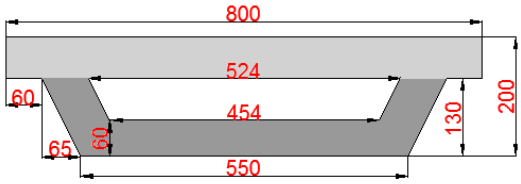

(e) T-HBFW

Normal Strength Concrete

High Strength Concrete All Dimensions in mm

Figure (2): Continue.

Symbols used in specimen designation refer to: T: Trapezoidal cross section, H: High strength concrete, N: Normal strength concrete, UF: Upper Flange, BF: Bottom Flange, and W: Web.

T-HT: HSC at total (overall) depth of box girder.
T-NT: NSC at total (overall) depth of box girder.
T-HUF: HSC at upper flange only.
T-HUF0.5W: HSC at upper flange and half depth of the webs.
T-HBFW: HSC at bottom flange and total depth of the webs.

2.2 Materials

In manufacturing test specimens, the following materials have been used: ordinary Portland cement (Type 1); rounded gravel with maximum size of (10mm); natural sand from AL-Ukhaider region, Karbala, Iraq, high water reducer superplasticizer (Flocrete PC200), limestone powder (LSP) has been used for self-compacting concrete (SCC) mix (SCC was used due to small dimensions of box girder section and relatively dense reinforcement), and clean tap water has been used for both mixing and curing. Two concrete mixes have been designed in this study (NSC and HSC). The compressive strengths of NSC and HSC were about 35 MPa and 55 MPa respectively at 28 days age. The concrete mix properties are reported and presented in Table (1).

Also, the yield strength of steel (f_y) for bar size (10 and 6) mm was (520 and 580) MPa, respectively with the value of modulus of elasticity (E_s) was taken as (200 GPa) for all sizes.

Table (1): Mix Proportion of concrete

Materials (kg/m^3) / Mixes	Cement	LSP	Gravel	Sand	Water	SP*	W/C	W/P **
NSC	430	120	800	790	200	8	0.465	0.364
HSC	470	125	800	790	157	12.5	0.334	0.264

* SP = Superplasticizer
** W/P = Water/ Powder (sand + gravel)

2.3 Testing

Five simply supported box girders specimens loaded transversely by two line load applied at points of third span (the distance of third span equal to 680 mm) were tested by using a hydraulic universal testing machine, in the structural laboratory of the college of engineering, Babylon University. Before testing, two strips 10 cm width and 6 mm thick rubber were placed between line loads and concrete face to avoid early crushing of concrete and another two strips 13 cm width rubber were placed between the concrete face and supports to avoid local failure. Also, two dial gages were used to read deflection, first dial gage under the mid span of the specimen and second dial gage under the load. Figure (3) shows the test specimen' setup.

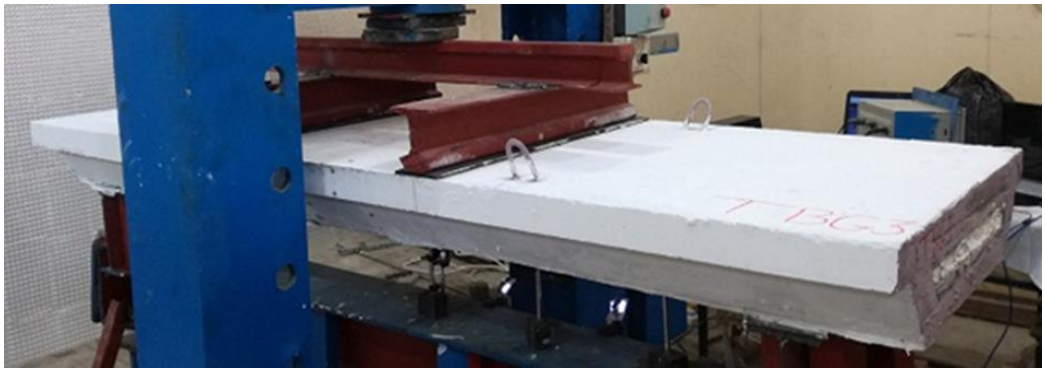

Figure (3): Test specimen' setup.

2.4 Experimental Results

The main objective of the present work is devoted to examine and study the effect of concrete hybridization technique on the structural behavior of reinforced concrete box girder. The overall behavior of box girders specimens were investigated and discussed in the following paragraphs.

2.4.1 Cracking Patterns and Ultimate Loads

As load increased gradually up to failure, the cracks that appeared on the specimen were mentioned and the corresponding loads were recorded. There are three types of develops cracks: flexural cracks, flexural-shear cracks, and inclined (diagonal) shear cracks.

2.4.1.1 Specimen T-HT

This specimen was made from HSC for overall section (upper flange, bottom flange and webs). The first flexural crack appeared at load 41 kN (i.e. at 14.8% of the ultimate load) in the bottom flange. Flexural cracks continued to appear in the web and bottom flange in the constant moment region until load 95 kN, at which first flexural shear crack was observed. At load about 118 kN, inclined shear cracks began to appear. The collapse occurred suddenly by crushing of concrete in the compression zone at mid span between the loads (formed a plastic hinge) at load about 277 kN. Figure (4) shows the failure mode of specimen T-HT.

Figure (4): failure mode of T-HT.

2.4.1.2 Specimen T-NT

This specimen was made of NSC for overall section (upper flange, bottom flange and webs). At load about 30 kN, first flexural crack was observed in the bottom flange at constant moment region (i.e. at 14.7% of the ultimate load) and at load 96 kN, first inclined shear crack appeared. The failure occurred due to yielding of steel reinforcement in the tension zone (tensile flexural failure) after wide expand of flexural cracks at bottom flange at load 204 kN. When comparing T-NT with T-HT, the first cracking load of T-HT greater than the first cracking load of T-NT by about 37%, this increase in the amount of cracking load is due to increase in the modulus of rupture of T-HT. In addition, the box girder T-HT has ultimate load capacity higher than the box girder T-NT by about 36%. Figure (5) shows the failure mode of specimen T-NT.

Figure (5): Failure mode of T-NT.

2.4.1.3 Specimen T-HUF

This specimen was made from HSC in the upper flange and from NSC in webs and bottom flange. First crack that observed was a flexural crack in the bottom flange at load 35 kN (approximately 14.5% of ultimate load) , it is higher than cracking load of T-NT by about 16.7%, this increasing due to increase in the tensile strength of concrete, and lower than T-HT by about 17% because T-HUF has NSC in most areas of tension zone. With load increasing, flexural, flexural shear, and inclined cracks (shear crack) appeared along the box girder specimen with each stage of loading. The failure due to the yield of steel reinforcement in the tension zone (tensile flexural failure) at load 241 kN. In comparison with homogenous box girders, it was noticed that T-HUF has ultimate load capacity higher than T-NT by about 18% and lower than T-HT by about 13%. Figure (6) shows the failure mode of specimen T-HUF.

Figure (6): Failure mode of specimen T-HUF.

2.4.1.4 Specimen T-HUF0.5W

This specimen was made from HSC in upper flange and half depth of the webs and from NSC in the other half of the webs and bottom flange. At load 35 kN (approximately 13.3% of ultimate load), first flexural crack appeared in the constant moment region as the same as the specimen T-HUF. While loading increasing, the way that appeared cracks (flexural, flexural-shear, and inclined shear) in which the same as specimen T-HUF but in higher loads due to the existence of HSC in half depth of the web. In addition, the failure occurred due to yield steel reinforcement in the tension zone (tensile failure) at load 263 kN like the failure of T-HUF but in ultimate load capacity higher than T-HUF by about 9.1%. Figure (7) shows the failure mode of specimen T-HUF0.5W.

Figure (7): failure mode of specimen T-HUF0.5W.

2.4.1.5 Specimen T-HBFW

This specimen was made from HSC in the webs and bottom flange and from NSC in the upper flange. At load 40 kN (approximately 16% of ultimate load), the first crack (it was a narrow flexural crack) was observed in the bottom flange under the load. In comparison with homogenous specimens, the first cracking load of T-HBFW is higher than T-NT by about 33% and lower than T-HT by only about 2.5%. This amount of cracking load is due to use of high strength concrete in most areas of tension zone (webs and bottom flange). At load about 189 kN, longitudinal cracks in the top flange were observed starting from the supports towards the loads. Finally, failure occurred suddenly at load 250 kN due to crushing of concrete in the bottom flange and top flange. This type of failure in this specimen may be it happened due to transverse bending stresses caused by the moments at the web-upper flange junction. In comparison with homogenous box

girders, T-HBFW has ultimate load capacity higher than T-NT by about 22.5% and lower than T-HT by about 10%. Figure (8) shows the failure mode of specimen T-HBFW.

Figure (8): Failure mode of specimen T-HBFW.

2.4.2 Load – Deflection Curve

In general, there are three stages of load-deflection response, these are: elastic-uncracked, elastic-cracked and ultimate stage, where the first stage terminates when the cracks develop. In elastic-uncracked stage, deflection increase linearly in all beams with loading since the materials in compression and tension zone are in elastic manner. In elastic-cracked (post-cracking) stage there is also linear relationship between load and deflection but with a reduction in slope. After this stage, the slope decrease largely and aggravated increments in deflection to small increase in loading level up to failure.

Through the testing two dial gages were used, one of them was put at mid span and the other was put at one-third span (under the load) to study the behavior of the tested specimens through load-deflection relationships. Figure (9) shows the Effect of hybrid technique on the load-deflection curve for trapezoidal box girders specimens.

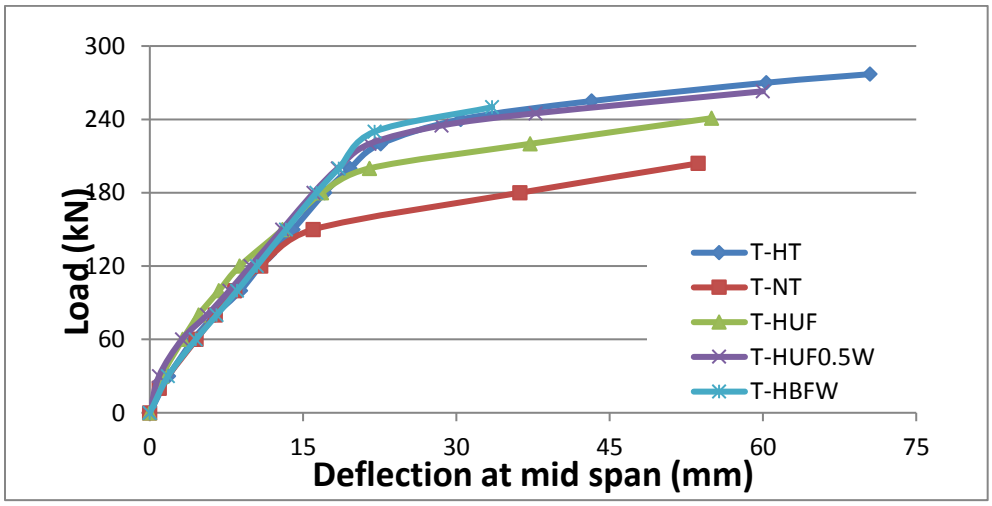

Figure (9): Effect of hybrid technique on the load-deflection curve for trapezoidal box girders specimens.

Table (2): Experimental results of the tested specimens.

Specimen	Applied load (kN)		Mid span deflection (mm)			Failure mode
	P_{cr}	P_u	Δ_{cr}	Δ_s*	Δ_u	
T-HT	41	277	2.42	17.13	70.49	Typical flexural failure
T-NT	30	204	1.94	15.21	53.66	Typical flexural failure
T-HUF	35	241	2.27	13.96	55.33	Typical flexural failure
T-HUF0.5W	35	263	2.12	15.81	61.63	Typical flexural failure
T-HBFW	40	250	2.06	14.33	33.12	Local transverse flexural

* deflection at service load (0.65 of ultimate load)

3. Numerical Analysis

The aim of this section is to check the validity and accuracy of the numerical model of the hybrid reinforced concrete box girder, which constructed from two different types of concrete (NSC and HSC).

This chapter includes a nonlinear finite element analysis for the tested box girders. The analysis was done by using ANSYS software (version 16.1, 2015).

3.1 Description of Box Girders Specimens in Finite Element

By using the advantage of the symmetry for box girder geometry, loadings, and supporting a quarter of box girder was used for finite element analysis, as shown in Figure (10) and Figure (11).

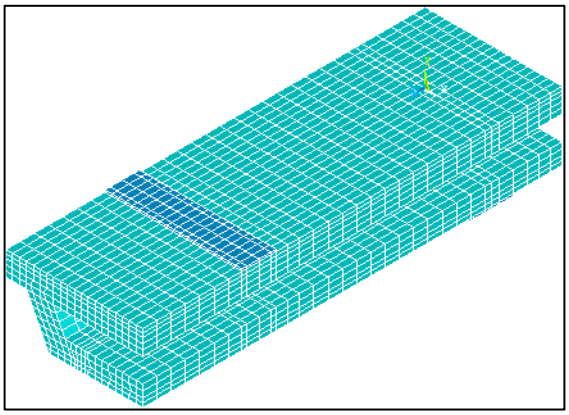

Figure (10): Quarter of trapezoidal box girder

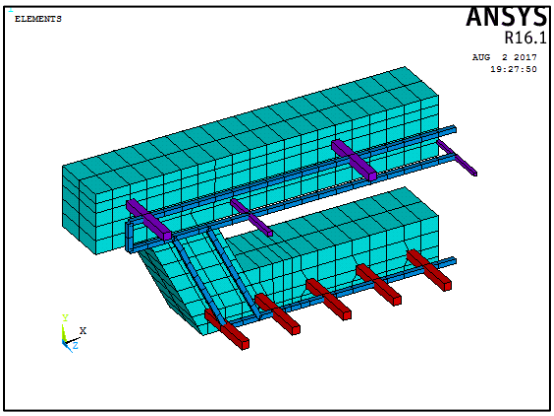

Figure (11): Typical cross-section

An important step in finite element modeling is the selection of the mesh density. A convergence of results is obtained when an adequate number of elements are used in a model. This is practically achieved when an increase in the mesh density has a negligible effect on the results. Therefore, in this finite element modeling, a convergence study is carried out to determine an appropriate mesh density. Four types of mesh are used to find the best mesh size for the homogenous box girder (T-NT).

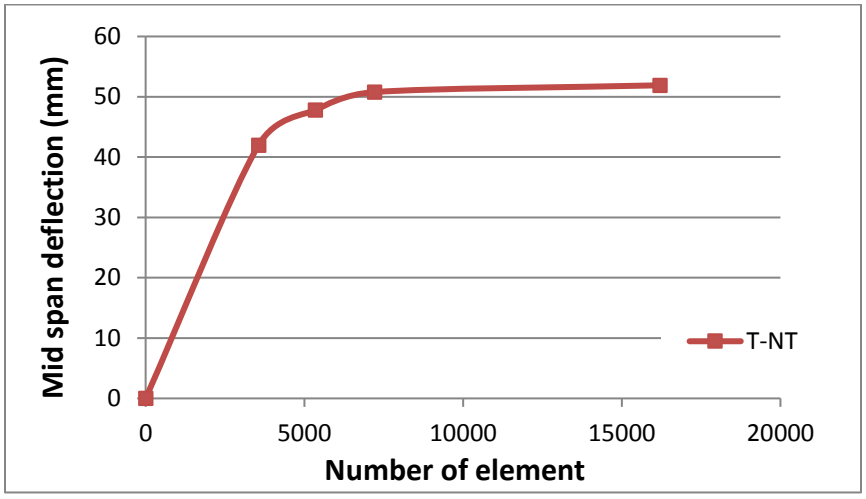

Figure (12): Convergence study of present box girders.

From Figure (12), it can be observed that the increased number of elements from (7208) to (16205) had a negligible effect on maximum deflection; therefore, the mesh with number of elements (7208) was selected for model T-NT.

3.2 Modeling of Reinforced Concrete Box Girder Specimen

For modeling the homogenous and hybrid box girders, a solid element (solid 65) was used to model the concrete in two types high strength (HSC) and normal strength (NSC), a solid element (solid185) was used to model loading and base plates, and (link 180) was used to model steel reinforcement.

Boundary conditions (BC) were need to apply at points of symmetry, where the supports and loads exist. To model the symmetry, nodes on these planes must be constrained in the perpendicular directions. Therefore, the nodes of mid- span plane must be restricted in x-direction and y- direction, and the nodes in longitudinal plane must be restricted in x-direction only. The support was modeled in such a way as a roller. A single line of nodes on the plate is given constraint in the Uy direction. By doing this, the beam will be allowed to rotate at the support. Figure (13): shows the details of BC of the quarter symmetry of box girder

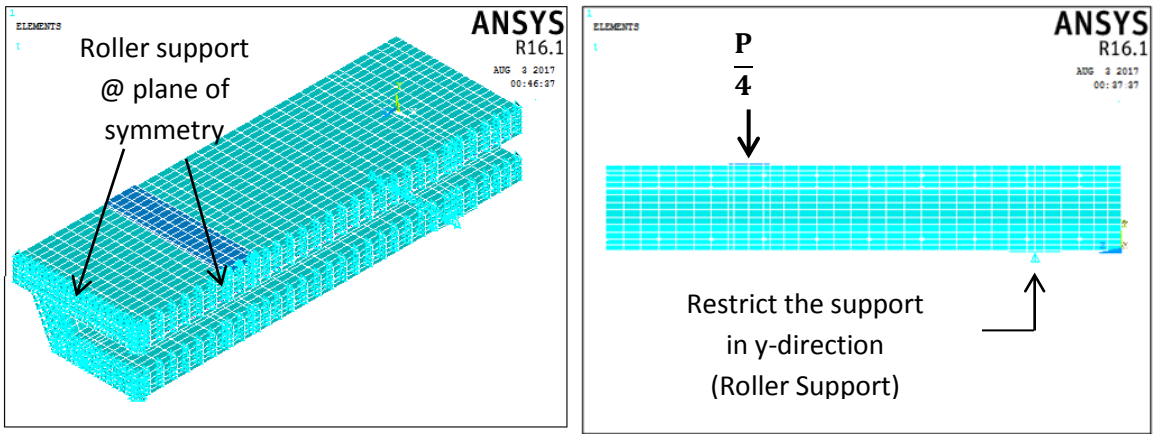

Figure (13): Details of BC of the quarter symmetry of box girder.

The external distributed applied load was represented by dividing the total distributed load on the top nodes according to area rounded of each node to represent the distributed load in ANSYS program.

3.3 Results of Finite Element Analysis

All tested box girders were analyzed by using a computer program (ANSYS-16.1), as mentioned previously. This comparison includes: first cracking load, cracking patterns, ultimate load and ultimate deflections at mid-span.

3.3.1 First Cracking Load

Table (3) shows the comparison between experimental and numerical results for the first cracking load .

Table (3): Experimental and numerical results for first cracking load.

Specimen	First cracking load (kN)		
	Experimental $P_{cr(EXP.)}$	Numerical $P_{cr(FEM)}$	$\frac{P_{cr(FEM)} - P_{cr(EXP.)}}{P_{cr(EXP.)}} \times 100\%$
T-HT	41	47	14.63%
T-NT	30	33	10%
T-HUF	35	39	11.43%
T-HUF0.5W	35	40	14.29%
T-HBFW	40	43	7.5%
-	-	-	Average = 8.712%

Table (3) shows that the first cracking $P_{cr(FEM)}$ in all numerical models of box girder is greater than that $P_{cr(EXP.)}$ in experimental specimens and the percentages of difference are between (7.5 – 14.63)%.

3.3.2 Ultimate Load

Table (4) shows another comparison between experimental and numerical results for the ultimate load.

Table (4): Experimental and numerical results for ultimate load.

Specimen	Ultimate load (kN)		
	Experimental $P_{u(EXP.)}$	Numerical $P_{u(FEM)}$	$\frac{P_{u(FEM)} - P_{u(EXP.)}}{P_{u(EXP.)}} \times 100\%$
T-HT	277	289	4.33%
T-NT	204	214	4.9%
T-HUF	241	247	2.49%
T-HUF0.5W	263	269	2.28%
T-HBFW	250	254	1.6%
-	-	-	Average = 3.12%

Table (4) shows that the ultimate load $P_{u(FEM)}$ in all numerical models of box girder is greater than that $P_{u(EXP.)}$ in experimental specimens and the percentages of difference are between (1.6%- 4.9%).

3.3.3 Ultimate Deflection

The ultimate deflections (vertical displacements) were measured at mid-span at the center of the bottom face of the bottom flange of box girder. A comparison was made between experimental and numerical results of mid span ultimate deflection as shown in Table (5).

Table (5): Experimental and numerical results for ultimate deflection.

Specimen	Ultimate deflection (mm)		
	Experimental $\Delta_{u(EXP.)}$	Numerical $\Delta_{u(FEM)}$	$\frac{\Delta_{u(FEM)} - \Delta_{u(EXP.)}}{\Delta_{u(EXP.)}} \times 100\%$
T-HT	70.49	67.27	-4.57%
T-NT	53.66	50.78	-5.37%
T-HUF	55.33	49.82	-9.96%

Table (5): Continue

T-HUF0.5W	61.63	54.57	-11.46%
T-HBFW	33.12	27.63	-16.58%
-	-	-	Average = -9.588%

The comparison of Table (5) for the ultimate deflection at mid span shows that the deflection in numerical models is in general smaller than that in experimental samples.

3.3.4 Load Deflection Curve

Figure (14) shows a comparison between the experimental and numerical results related to load and deflection for all the specimens of the present study.

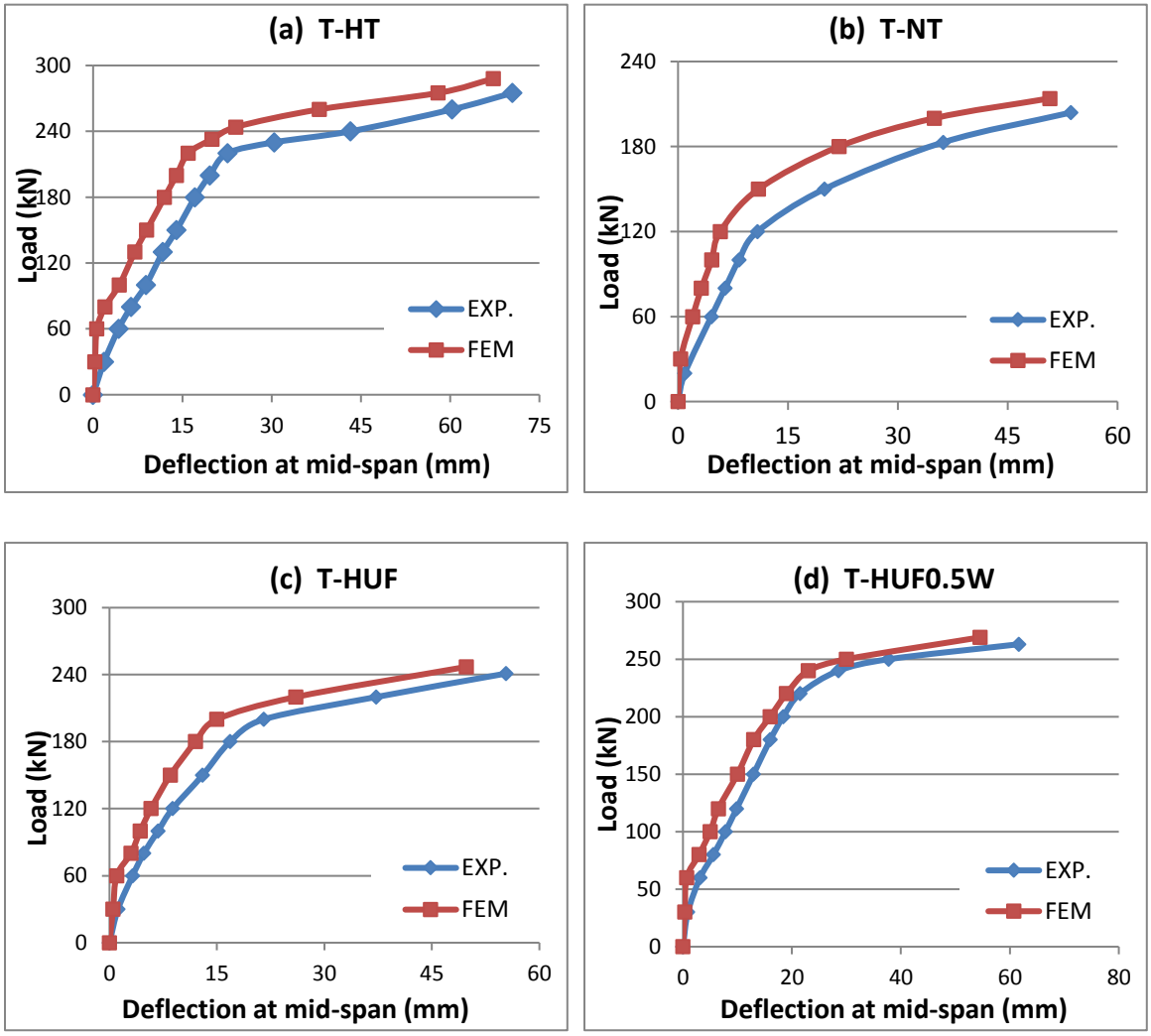

Figure (14): Experimental and numerical load-deflection curves.

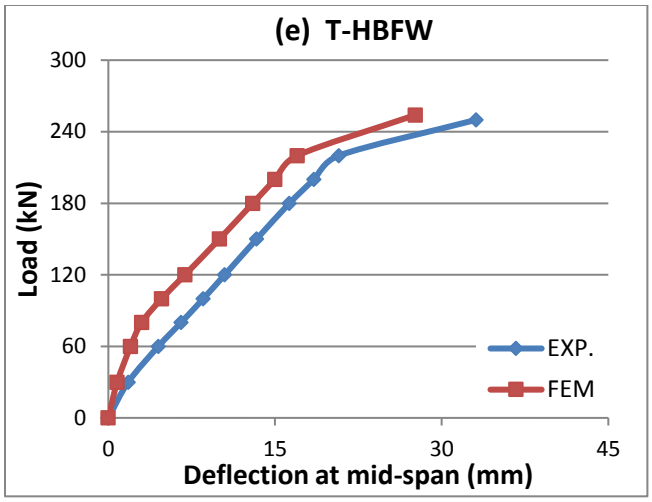

Figure (14): Continue.

From previous curves, a relatively stiffer numerical response has been observed at the advanced stages of loading. As a general response, the load deflection plots for the beams from the finite element analysis gave an acceptable agreement when compared with the experimental data, where the three stages of load-deflection response (elastic-uncracked, elastic-cracked and Elasto-plastic) can be noticed.

4. Conclusion

4.1 Experimental Work

1. The ultimate load of hybrid trapezoidal box girder specimens increased by about (18, 29, and 23) % when using HSC in the upper flange, upper flange and half depth of webs, and bottom flange with total depth of webs respectively.

2. Hybrid technique caused increases in first cracking load about (17- 33) % in comparison with homogenous specimen (full NSC).

3. The location of HSC layer had a significant effect on the failure shape of trapezoidal box girders.

4. The ultimate load for high strength trapezoidal specimens is higher than the hybrid specimens by not more than 9%. This means that hybridization may be effective and economical.

4.2 Numerical Analysis

1. A comparison between the results (first cracking loads, ultimate loads, load- deflection curves, and failure modes) of numerical analysis by (ANSYS V16.1) and experimental work showed an acceptable agreement with difference about (3.12% and 9.588%) as average for ultimate load and ultimate deflection, respectively .

2. First cracking load and ultimate load that found from numerical analysis were higher than that found from experimental work with maximum difference 14.63% and 4.9% respectively.

3. Through the comparison among all hybrid trapezoidal box girders, the specimens that made from HSC in upper flange and total depth of webs are the best. This specimens have the highest ultimate load and the highest stiffness in compare with other hybrid specimens.

References

AASHTO, Fifth Edition 2010, "AASHTO LRFD Bridge Design Specifications". American Association of State Highway and Transportation Officials, USA.

Ansys, "ANSYS Help", Release 16.1, copyright 2016.

Ashour S.A., and Wafa F.F. , May-June 1993, "Flexural Behavior of High Strength Fiber Reinforced Concrete Beams", ACI Structural Journal, Vol. 90, No. 3, pp. 279-287.

Newman, J., and Choo, B.S., 2003, "Advanced Concrete Technology", Edition, Elsevier Ltd., UK (616) p.

Paval M.E; B, 2016, "Analysis of Multi-Cell Prestressed Concrete Box-Girder Bridge", International Journal of Engineering Technology Science and Research IJETSR, Volume 3, Issue 4.

Upadhyay A. and Maru S., 2017, "Comparative Study of PSC Box Girder Multi Cell (3-Cell) Bridge of Different Shapes: A Review Paper", Global Research and Development Journal for Engineering, Volume 2.